

## Columnar AlGaIn/GaN Nanocavities with AlN/GaN Bragg Reflectors Grown by Molecular Beam Epitaxy on Si(111)

Jelena Ristić,<sup>1,\*</sup> Enrique Calleja,<sup>1</sup> Achim Trampert,<sup>2</sup> Sergio Fernández-Garrido,<sup>1</sup>  
Carlos Rivera,<sup>1</sup> Uwe Jahn,<sup>2</sup> and Klaus H. Ploog<sup>2</sup>

<sup>1</sup>*ISOM and Departamento de Ingeniería Electrónica, Universidad Politécnica de Madrid, Madrid, Spain*

<sup>2</sup>*Paul-Drude-Institut für Festkörperelektronik, Berlin, Germany*

(Received 28 October 2004; published 12 April 2005)

Self-assembled columnar AlGaIn/GaN nanocavities, with an active region of GaN quantum disks embedded in an AlGaIn nanocolumn and cladded by top and bottom AlN/GaN Bragg mirrors, were grown. The nanocavity has no cracks or extended defects, due to the relaxation at the Si interface and to the nanocolumn free-surface to volume ratio. The emission from the active region matched the peak reflectivity by tuning the Al content and the GaN disks thickness. Quantum confinement effects that depend on both the disk thickness and the inhomogeneous strain distribution within the disks are clearly observed.

DOI: 10.1103/PhysRevLett.94.146102

PACS numbers: 81.16.Dn, 78.55.Cr, 78.67.Bf, 81.15.Hi

The wide interest in blue and UV-range optoelectronic devices has spurred extensive scientific and technological effort into the field of III nitrides. Because of their direct wide band gap, GaN and its alloys with In and Al are not only suitable for detectors [1], light emitting diodes [2], and vertical cavity surface emitting lasers [3] for a broad variety of applications, but also envisaged as an excellent material system for fabrication of semiconductor microcavities. Compared to GaAs quantum microcavities, the expected Rabi splitting (splitting of exciton-polariton modes) is predicted to be more than an order of magnitude higher, due to a giant exciton oscillator strength in GaN [4].

In addition, an overall improvement of the optoelectronic devices is anticipated through further miniaturization to nanoscale dimensions that enhances charge localization effects. In that direction, attempts to achieve “wire-like” nanostructures, either by a self-assembled process or by electron-beam lithography definition, are pursued [5–7]. The growth of self-assembled III-nitride nanocolumns by molecular beam epitaxy (MBE) on different substrates has been recently reported [7–9]. These nanocolumns are fully relaxed and free of extended defects, showing excellent optical properties. The columns diameter (20–120 nm) and density are successfully controlled by means of the III/V element flux ratio and the growth temperature [7]. Once the nanocolumnar growth is mastered, different heterostructures with additional lateral confinement can be grown by placing quantum disks of a lower band gap material, like the GaN/AlGaIn nanostructures already reported [10]. Such structures are especially attractive for single photon sources [11], for parametric amplifiers or switches, and for developing novel devices such as single electron transistors or highly sensitive biosensors.

In this Letter we report on the self-assembled growth by MBE of columnar GaN/AlGaIn nanocavities on Si(111) substrates. This approach allows the fabrication of bottom-up freestanding nanodimensional optical devices without

any additional postgrowth processing. The nanocavity active region consists of GaN multiple quantum disks (MQD) embedded in an AlGaIn nanocolumn. The nanocavity was achieved by cladding the active region with top and bottom AlN/GaN distributed Bragg reflectors (DBR) with layer thicknesses fit to a quarter-wave rule ( $n_i d_i = \lambda/4$ ),  $\lambda$  being the cavity mode wavelength. In spite of the fact that the average nanocolumn diameter (20–60 nm) is comparable to the nanocavity mode wavelength, so that lateral confinement effects should not be neglected, the cavity mode was assumed, as a first approximation, to be a plane wave and the active region thickness was set to  $\lambda/2$ . Quantum confinement effects were studied by low temperature photoluminescence (PL) and cathodoluminescence (CL) (Zeiss DSM 962 Mono-CL system). The nanocavity structural quality and geometry was assessed by transmission electron microscopy (TEM).

AlGaIn nanocolumns with a 28% Al mole fraction were grown by plasma-assisted MBE under N-rich conditions on Si(111) substrates [12]. Subsequently, a series of 5 GaN MQD of different thicknesses, embedded in AlGaIn nanocolumns, were grown by simple interruption of the Al flux during the AlGaIn growth.

PL spectra of the above-mentioned GaN/AlGaIn MQD samples, with 2, 3, and 4.25 nm thick GaN disks, together with a spectrum of a single AlGaIn nanocolumn with the same Al content (reference sample, m1077), are shown in Fig. 1. The emission from the GaN MQD blueshifts with decreasing QD thickness and both the trend and the energies involved agree well with the calculated values that will be published elsewhere. Thus, for a given Al content of the AlGaIn barrier layers, the emission energy can be tuned by changing the GaN disk thickness.

In order to grow the full nanocavity structure, a stack of 3 nm thick GaN MQD (sample m1085) emitting at 3.591 eV (345.4 nm) was chosen for the active region. The total heterostructure thickness, including the DBR,

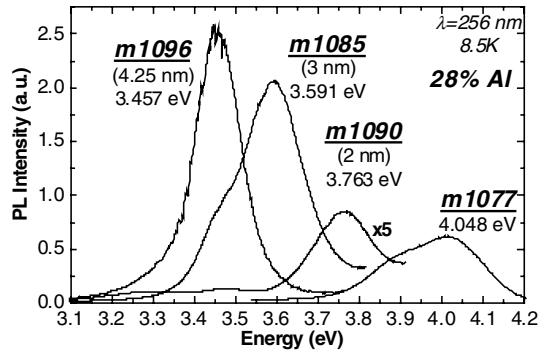


FIG. 1. PL spectra of nanocolumnar  $\text{Al}_{0.28}\text{Ga}_{0.72}\text{N}$  reference sample and various nanocolumnar  $\text{AlGaIn}/\text{GaN}$  heterostructures comprising 5 GaN MQD of different thicknesses.

was set to  $\lambda/2$  (172.7 nm). Given the rather small  $\text{AlGaIn}/\text{GaN}$  refractive index contrast ( $\Delta n = 0.14$  for 28% Al), a high reflectivity DBR based on these materials needs either a high number of bilayer periods or a high Al mole fraction. Under these conditions a network of cracks develops in compact planar DBR due to the lattice and thermal mismatch induced tensile strain [13]. However, crack formation is not expected to happen in  $\text{AlGaIn}$  nanocolumns that are strain-free due to the lattice and thermal relaxation at the interface with the substrate [14], and the DBR built-in strain is to be reduced through the free surface (high surface to volume ratio). Top and bottom DBR, with reflectivities of 50% and 90%, are obtained with 6 and 11 periods of  $\text{AlN}/\text{GaN}$  bilayers (32/40 nm). The schematic diagram and the corresponding cross-section TEM image of the nanocavity structure are shown in Fig. 2.

CL measurements in Fig. 3 show the nanocavity emission peak at 3.548 eV, in good agreement with the targeted nanocavity wavelength, even when the lateral confinement in the nanocavity active region is neglected.

The rather broad cavity emission (Fig. 3), as well as that from uncoupled GaN MQD heterostructures (Fig. 1), is mainly due to an inhomogeneous strain distribution within

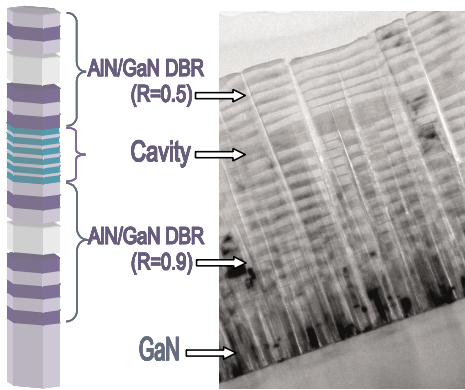


FIG. 2 (color online). Left: Scheme of the nanocavity structure (the white colored disks within the DBR mean “and so on”). Right: Cross-sectional TEM image of the actual nanocavity structure.

the GaN MQD. The accumulated elastic energy in pseudomorphically grown GaN disks on  $\text{AlGaIn}$  nanocolumns is gradually reduced towards the free surface along the disk radius. The lateral layer bending, shown in Fig. 4(b), may be due to this effect. The strain tensor equation, solved for the corresponding boundary conditions (pseudomorphic, 4 nm thick, GaN MQD grown on strain-free  $\text{AlGaIn}$  columns with 20% Al content, laterally surrounded by air) gives the in-plane compressive biaxial strain distribution (Fig. 5).

The strain effect on the PL emission energy is twofold: first, the strain induces bandgap changes, and, second, the strain-dependent piezoelectric field modifies the QD potential profile. These two effects depend on the QD thickness in opposite ways, as it is deduced from the theoretical estimation of the ground state (e1-hh1) transition energies derived from

$$E_G^{\text{eff}}(x=0) = E_G^{\text{strain}}(\text{GaN}) + E^{\text{conf}} - eF_{\text{tot}}^{\text{strain}}w, \quad (1)$$

$$E_G^{\text{eff}}(x=r) = E_G^{\text{relaxed}}(\text{GaN}) + E^{\text{conf}} - eF_{\text{tot}}^{\text{relaxed}}w \quad (2)$$

for the center and the lateral free surface of a QD with radius  $r$ , respectively.  $E_G^{\text{strain}}(\text{GaN})$  is calculated from the bandgap energy dependence on the biaxial strain [15], and  $E^{\text{conf}}$  represents the confined electron and hole states energy difference within the QD, which depends on  $1/w^2$ ,  $w$  being the QD width.  $F_{\text{tot}}$  is the total electric field in the QD and  $[eF_{\text{tot}}w]$  accounts for the quantum confinement Stark effect (QCSE) when a very high electric field is present [16]. The relative weights of the terms  $E_G^{\text{strain}}(\text{GaN})$  and  $[eF_{\text{tot}}w]$  in Eqs. (1) and (2) are quite different, depending on the QD thickness, as it will be shown in detail elsewhere.

The reduced strain at the QD free surface annihilates partially the piezoelectric field, giving rise to a *new* carrier confinement mechanism (*strain confinement*), that depends on the QD thickness. This specific confinement mechanism is the origin of the luminescence quenching in very thin GaN QD, as well as the main source for the emission linewidth broadening observed in spectra of Fig. 1.

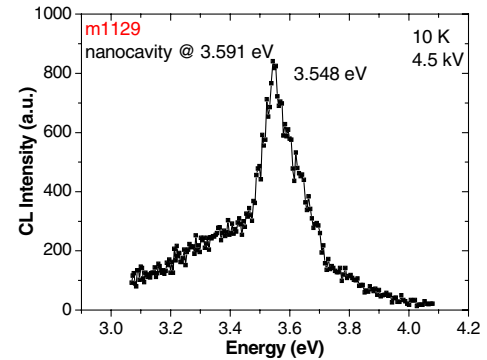


FIG. 3 (color online). Low temperature CL emission of the nanocavity.

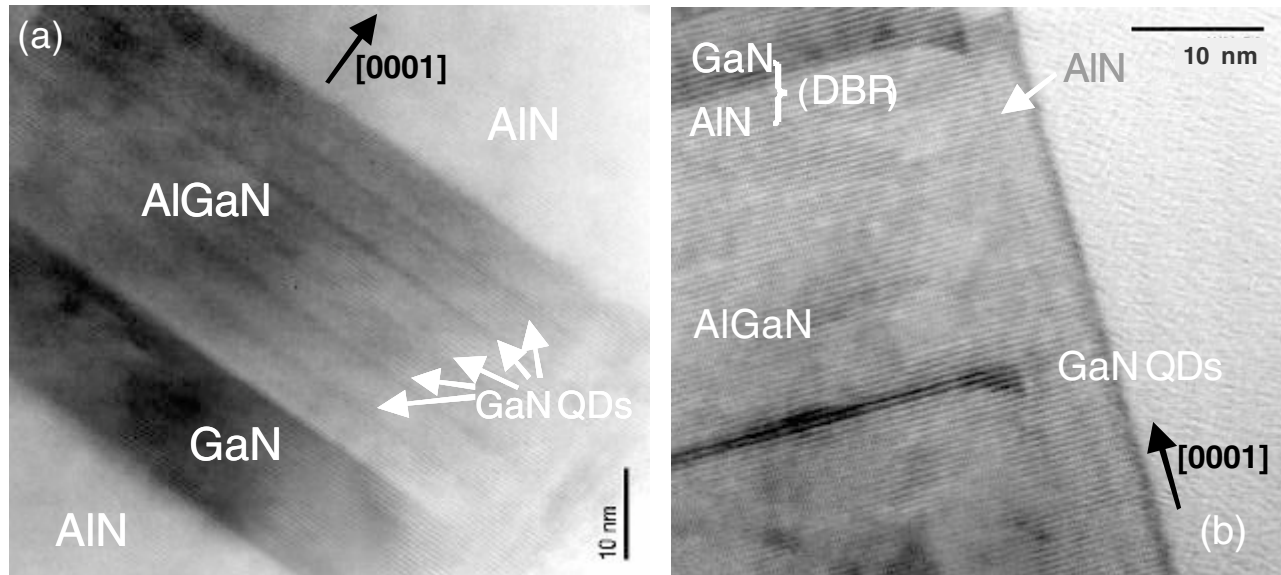


FIG. 4. High resolution TEM images of (a) the cavity area surrounded by the AlN/GaN DBR, and (b) the enhanced lateral growth effect on the nanostructure diameter.

Indeed, the energy broadening of the PL emission, considering the two extreme cases of full strain (disk center) and zero strain (disk free surface), is estimated to be 100 meV, in agreement with the experimental value.

The structural characterization of the nanocavity, provided by TEM measurements, shows the nanocavity active region with five GaN disks and the bottom 11-period DBR (Fig. 2). The disorder observed in the DBR region of the nanocavities is a result of lateral growth enhancement during the growth of the AlN/GaN stacks (Fig. 4). This lateral growth enhancement progressively increases the nanocolumn diameter, giving rise to different bilayers' thicknesses, so that the periodicity of the DBR is deteriorated, and eventually the nanocolumns lateral coalescence occurs. As a result, there is a layer geometry dispersion among different nanocavities (Fig. 2). The CL signal asymmetry in Fig. 3 is not just due to the plane wave approximation, but rather is a result of the DBR stop band asymmetry, caused by the geometry distortion.

The lateral growth enhancement is a consequence of nonoptimized DBR growth conditions, during uninterrupted growth of the entire nanocavity structure. The AlGaIn is grown at the optimal growth temperature for GaN nanocolumns, by replacing part of the Ga flux with Al while keeping the total III element flux constant. The lower thermal desorption rate of Al, as compared to that of Ga, results in an increase of the effective III/V ratio at the growth front, departing from the N-rich regime required. The situation becomes even worse when growing AlN. Namely, the growth "windows" (III/V flux ratio and growth temperature) for optimal GaN and AlN columnar growth are extremely narrow and barely overlapping, so that the optimization requires a careful selection of the growth conditions. It needs further readjustment of the III/V flux ratio or an increase of the growth temperature.

High growth temperatures, adequate for AlN, call for very high Ga flux, to compensate for the strong desorption that dramatically reduces the growth rate. In parallel, N flux must be high enough to ensure the needed N-rich regime for nanocolumn growth.

In summary, GaN/AlGaIn nanocavities were successfully grown on Si(111) by MBE. The heterostructures have an active region consisting of GaN MQD embedded in an AlGaIn nanocolumn and cladded by AlN/GaN DBR. Quantum confinement effects that depend on both the disk thickness and the inhomogeneous strain distribution within the disks are clearly observed. In spite of the heterostructures' geometry distortion due to undesired lateral growth enhancement, the nanocavity emission matches well the targeted GaN MQD emission. The enhancement of the lateral growth should be suppressed by optimization of the growth conditions for nanocolumnar AlN. To our

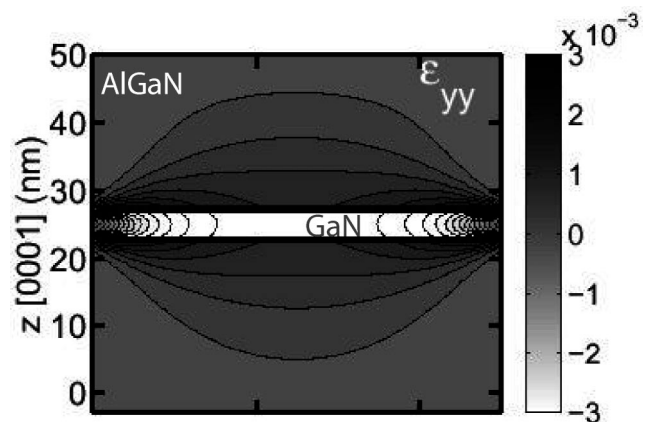


FIG. 5. In-plane strain distribution within a 4 nm thick GaN disk pseudomorphically grown on a strain-free AlGaIn nanocolumn with 20% Al content.

knowledge, this is the first report on self-assembled GaN/AlGaIn columnar nanocavities grown by MBE that may open the way to a broad range of applications in new optoelectronic devices. Moreover, these results may be effectively transferred to other material systems, thus, avoiding laborious technological processing, such as laser ablation or reactive ion etching that induces crystalline damage and surface states.

The authors acknowledge Professor Aldo di Carlo and Michael Povolotskyi for the strain distribution simulations and thank Professor Carlos Tejedor and Professor Jose Manuel Calleja for the fruitful discussions. Partial financial support was provided by Spanish Ministry of Education and Science Project No. MAT 2004-02875 and Autonomous Community of Madrid Project No. GR/MAT/0042/2004.

---

\*Permanent address: Universidad Rey Juan Carlos, Dpto. Cc. de la Comunicación, E-28943 Fuenlabrada, Madrid, España.

Electronic address: jelena@die.upm.es

- [1] Z.C. Huang, J.C. Chen, D.B. Mott, and P.K. Shu, *Electron. Lett.* **32**, 1324 (1996).
- [2] S. Nakamura, M. Senoh, S.I. Nagahama, N. Iwasa, T. Yamada, T. Matsushita, H. Kiyoku, Y. Sugimoto, T. Kozaki, H. Umemoto, M. Sano, and K. Chocho, *Appl. Phys. Lett.* **72**, 2014 (1998).
- [3] S. Nakamura and G. Gasal, *The Blue Laser Diode* (Springer-Verlag, Berlin, 1998).
- [4] A. Kavokin and B. Gil, *Appl. Phys. Lett.* **72**, 2880 (1998).
- [5] Z.H. Wu, X. Mei, D. Kim, M. Blumin, H.E. Ruda, J.Q. Liu, and K.L. Kavanagh, *Appl. Phys. Lett.* **83**, 3368 (2003).
- [6] Z.L. Wang, X.Y. Kong, and J.M. Zuo, *Phys. Rev. Lett.* **91**, 185502 (2003).
- [7] E. Calleja, M.A. Sánchez-García, F.J. Sánchez, F. Calle, F.B. Naranjo, E. Muñoz, U. Jahn, and K.H. Ploog, *Phys. Rev. B* **62**, 16 826 (2000).
- [8] S. Guha, N. Bojarczuk, M. Johnson, and J. Schetzina, *Appl. Phys. Lett.* **75**, 463 (1999).
- [9] M. Yoshizawa, A. Kikuchi, N. Fujita, K. Kushi, H. Sasamoto, and K. Kishino, *J. Cryst. Growth* **189–190**, 138 (1998).
- [10] J. Ristić, E. Calleja, M.A. Sánchez-García, J.M. Ulloa, J. Sánchez-Páramo, J.M. Calleja, A. Trampert, U. Jahn, and K.H. Ploog, *Phys. Rev. B* **68**, 125305 (2003).
- [11] E. Moreau, I. Robert, J.M. Gérard, I. Abram, L. Manin, and V. Thierry-Mieg, *Appl. Phys. Lett.* **79**, 2865 (2001).
- [12] J. Ristić, M.A. Sánchez-García, E. Calleja, J. Sánchez-Páramo, J.M. Calleja, U. Jahn, and K.H. Ploog, *Phys. Status Solidi A* **192**, 60 (2002).
- [13] S. Fernández, F.B. Naranjo, F. Calle, M.A. Sánchez-García, E. Calleja, A. Trampert, and K.H. Ploog, *Semicond. Sci. Technol.* **16**, 913 (2001).
- [14] A. Trampert, J. Ristić, U. Jahn, E. Calleja, and K.H. Ploog, in *Proceedings of the 13th International Conference on Microscopy of Semiconducting Materials*, edited by A. G. Cullis and P. A. Midgley, IOP Conf. Ser. No. 180 (Institute of Physics and Physical Society, London, 2003), p. 167.
- [15] K. Kim, W.R.L. Lambrecht, and B. Segall, *Phys. Rev. B* **50**, 1502 (1994); J.B. Jeon, B.C. Lee, Y.M. Sirenko, K.W. Kim, and M.A. Littlejohn, *J. Appl. Phys.* **82**, 386 (1997).
- [16] A. Bonfiglio, M. Lomascolo, G. Traetta, R. Cingolani, A. Di Carlo, F. Della Sala, P. Lugli, A. Botchkarev, and H. Morkoc, *J. Appl. Phys.* **87**, 2289 (2000); A. Hangleiter, *J. Lumin.* **87–89**, 130 (2000).